

REMOTE CONTROLLED NANOPARTICLE HEATING FOR BIOMEDICAL APPLICATIONS

Wen Dongsheng

School of Engineering and Materials Science,

Queen Mary University of London

London, E1 4NS

United Kingdom

E-mail: d.wen@qmul.ac.uk

ABSTRACT

Recent years see intensive interests in the synthesis and application of nanomaterials in different fields extending from energy to biomedicine sectors. Many biomedical applications involve delivering bio-modified nanoparticles to malignant cells and rapidly heating nanoparticles with an external source such as laser, ultrasound or an electromagnetic wave to produce a therapeutic effect or to release drugs. The interaction of nanoparticles with the external source and subsequent heating effect is fundamental for the successful deployment of these novel techniques. This study proposes a systematic study of remote-controlled nanoparticle heating for medical applications. Initial theoretical and experimental studies are conducted to reveal the potentials of this exciting field. The combination of gold nanoparticles with ultrasound irradiation or electromagnetic wave at radiofrequency spectrum has been shown to be a promising strategy for targeted medical applications.

KEYWORDS

Nanoparticle, heating, cancer therapy, electromagnetic, ultrasound

INTRODUCTION

Nanotechnology is the study of manipulating matter at an atomic or molecular scale where the quantum mechanical effect becomes important. It has been the major driven force of technological innovation in the last a few decades, and is expected to play a fundamental role in improving the quality of life and achieving sustainable development of the modern society. Intensive worldwide effort has been focused on this multi-disciplinary and far-reaching field. Though there is still much debate on the future implications of nanotechnology, much progress has been made from the creation of many new materials and devices to a vast range of applications, such as in electronics, biomaterials, medicine and energy utilization.

For medical applications, the use of nanotechnology could revolutionize the way we detect and treat damage to the human body and disease in the future. Many techniques only imagined a few years ago are making remarkable progress towards

becoming realities. The major applications of nanotechnology can be found in a wide spectrum from drug delivery, diagnostic and imaging process, therapeutic applications to anti-microbial and cell repairs. For instance, controlled drug release involves delivering functionalized nanoparticles containing drugs or other chemical species to targeted cells (i.e. cancer cells), where a localized release of therapeutic loads produces a treatment effect while minimizing the damage of surrounding healthy cells. For many of these applications, heat transfer plays a significant role. An optimised heating effect is fundamental to the successful employment of these applications, where a systematic investigation is still currently lacking.

This work conducts a review on the heating of nanoparticles by an external source such as ultrasound, laser, microwave, and electromagnetic field, and reports our latest development in the field theoretically and experimentally; especially the ultrasound and RF heated nanoparticle suspensions for targeted medical applications.

REMOTE CONTROLLED NANOPARTICLE HEATING FOR MEDICAL APPLICATIONS

Through many years, treatment by direct or indirect thermal therapy has been one of the most widely used methods in clinical practice. For instance the Radiofrequency Ablation (RFA) is based on the dielectric heat generated by an electromagnetic (EM) field. Clinically it requires a surgeon to insert a thin bundle of conducting wires into the malignant cells through a needle under imaging guidance. Despite its relative success, such a method has several limitations, such as the invasive nature of the treatment, incomplete destruction of large tumors (> 4–5 cm in diameter), thermal injury to normal tissues and applicability to non-metastatic tumors localized in relatively few sites (liver, kidney, breast, lung and bone).

As one of the building blocks of nanoscience and nanotechnology, various aspects of nanoparticles have been extensively investigated over the past few decades; significant advances have been made on chemistry and materials synthesis of new classes of nanoparticles. There is an emerging application of nanomaterials in medical and healthcare sectors,

i.e. controlled drug release [1], enhanced imaging and diagnosis [2], non-invasive hyperthermia treatment [3] and photothermal therapy (PTT) [4], to name but a few. For these applications, a typical process involves i) functionalisation of nanomaterials with targeting agency, ii) controlled delivery of these materials to targeted sites and iii) initiation of heat to produce a direct therapeutic effect (hyperthermia or PTT), to release drugs (controlled drug release) or to produce a different light reflection mode (imaging and diagnosis). An optimised heating effect is fundamental to these applications.

Heat can be introduced both remotely and non-remotely. Usually non-remotely introduced heating, such as through direct heating, exothermic reactions or RF probes as the example in RFA above, has an invasive nature. While it destroys malignant cells, it causes irreversible damage to surrounding health cells. Non-invasive treatment is therefore preferred. Different methods, including laser, electromagnetic (EM) wave, ultrasound and light, have been used to heat nanoparticles remotely. In many medical applications, localized heating of cells and tissues that achieves the therapeutic benefits while minimizing the collateral damage to nearby cells and tissue is highly desirable.

Currently there are two major research areas in using nanoparticles for thermal therapies: magnetic nanoparticle mediated hyperthermia [3,5,6] and photothermal therapy [7,8,9]. Compared to the laser or light treatment, therapy by electromagnetic waves (EM) in the radiofrequency (RF) spectrum has some distinctive advantages. RF is not ionization and the specific absorption rate (SAR) is strongly frequency-dependent. At low frequencies, RF can pass harmlessly through the body and heat only the nanoparticles. Such uniqueness offers a good opportunity for treatment of deep-seated tumors. Magnetic nanoparticles (NPs) both metal oxides and metals, such as Fe_2O_3 , Fe_3O_4 , Fe, Co and Ni have been proposed as potential agents for non-invasive hyperthermia applications, where heating is induced by an external EM fields in the RF [3,6,7] or microwave spectrum [10], or through an ultrasonic device [11]. However these magnetic nanoparticles generally have low SAR, typically in the range of 1~10 mJ/g nanoparticles [12] or equivalently ~500 W/g [13]. As a result it requires high concentration of nanoparticles under powerful magnetic field to have an effective treatment. The heat produced through the inductive coupling results in a temperature rise of typically a few degrees Celsius higher than body temperature in tens of minutes [3]. This slow temperature rise limits its effectiveness in treatment, as confirmed by a number of studies showing that re-growth of cancer cells was common (> 50%) when temperatures lower than 45°C are achieved [5]. For many applications, an ablative effect is desired ($T > 50^\circ\text{C}$).

Compared with nanoparticle mediated hyperthermia, photothermal therapy (PTT) through gold nanoparticles (GNP) has much high SAR due to their exceptional thermophysical and electrical properties. For PTT, heat is generated through the surface plasmon resonance (SPR) process due to the excitation of surface plasmons by light within a specific frequency range [8,9]. Such a process is a few orders of magnitudes higher in SAR than conventional light-sensitive dyes [9]. For PTT, only

small amount of gold nanoparticles is needed to achieve an ablative effect. However it suffers an inherent drawback, the resonance of gold nanoparticles is typically in the visible light (Vis) spectrum. Though by engineering the surface morphology of GNPs, i.e. gold nanorod, gold nanocage or gold nanoplate [8,9], the resonance wavelength can be shifted to near-infrared (NIR) spectrum, the scattering and attenuation of Vis-NIR light by biological tissues is still very strong. The treatment is limited by the penetration depth of the light and is therefore effective only for superficial tumors.

In addition, ultrasound method has been widely used in our daily life especially in medical diagnosis and treatment. It is also a versatile tool that can provide a means of thermal therapies extracorporally due to its deep penetration depth. Compared with other ways of treatment, ultrasound possesses the advantages of deep penetration length, flexible operation, easy-access and low cost. Its application, however, is generally limited by the damage of nearby health tissues and prolonged treatment time due to a relatively low heating or cavitation effect. While it destroys malignant cells, it causes damage to surrounding health cells. In many medical applications, localized, intensive heating through a non-invasive manner that achieves the therapeutic benefits while minimizing the collateral damage to nearby cells and tissue, is highly desirable. To address such issues, High Intensity Focused Ultrasound (HIFU) has been proposed as one of promising thermal therapies for deep-seated tumors such as prostate, liver, kidney, and breast [14]. HIFU propagates and focus ultrasonic beams to cause thermal injury in targeting sides. Diagnostic ultrasound is also generally built in HIFU to locate the target and monitor the treatment effects. Compared to Radiofrequency Ablation, HIFU is a minimal or no invasive treatment because there is no need for incision or probing physically into the tumor. Though successfully applied, there are still a few drawbacks of HIFU: i) The treatment duration is relatively long due to its small focus volume as the focus needs to be moved throughout the treatment; ii) The side-heating effect is still presenting, causing damage in healthy tissue surrounding the targeted sites and also changing the speed of sound, and iii) The alteration of sound speed distorts images in its diagnostic system, thus reducing the treatment effect. Further improvement of the HIFU has been investigated by a number of researchers [15,16]. A novel concept, nanoparticle-mediated ultrasonic therapy (NPUT), has been proposed recently in our group. The concept proposed to use nanoparticles to focus ultrasound energy and increase temperature locally and rapidly, which typically involves two processes, i) delivering nanoparticles to the target site, and ii) initiation of heat by ultrasound extra-corporally [17].

Above short review shows the potential of using heated nanoparticles for different biomedical applications. However as it shows, most of these studies have been conducted in medical fields where the focus is on the controlled delivery and cell effect. Though playing a crucial role in achieving the optimized treatment effect, there is still no systematic investigation of nanoparticle heating and its optimization, probably due to its multi-disciplinary nature, i.e. extending from medicine, nanotechnology to heat transfer studies. Next session will look into some principles of nanoparticle heating at analytical level.

NANOPARTICLE HEATING: THEORETICAL CONSIDERATION

The remote-controlled heating of nanoparticle suspensions typically involve two steps due to the large property difference between metallic nanoparticles and base fluids: 1) energy transfer from external source to nanoparticles and 2) heat transfer from nanoparticles to surrounding fluids. The temperature of nanoparticles is dependent on the power of the external source, which could induce two modes of heat flow from the nanoparticles to surrounding liquids, i) continuous heat flow (diffusion mode) occurs under low heat flux conditions or ii) discontinuous heat flow where bubbles could be formed around heated nanoparticles under high heat flux conditions. The first mode typically applies to ultrasound heating, RF hyperthermia with magnetic nanoparticles or heating induced by light-sensitive dyes. The second heat flow mode may occur under laser or ablative conditions. Below example analysis will be based on ultrafast lasers.

General consideration

For many laser-based applications, the time scale of laser pulses is comparable to that of energy carriers such as electrons and phonons. Table 1 summarizes various processes associated with ultrafast laser heating of metal nanoparticles [18]. The heating and heat dissipation from the nanoparticle to the surrounding occurs in a cascade of events. When the particle is exposed to an ultrafast laser pulse, free electrons absorb the energy of photons and increase their kinetic energy. These highly energetic electrons, having a nonequilibrium distribution of energy, are relaxed through electron-electron scattering on the order of 10-50 fs. Practically there is little energy exchange between electrons and phonons within this time scale and electron stay in a high energy level. The lattice temperature starts increasing as a result of electron-phonon scattering. A thermal equilibrium between the electrons and lattice is reached at tens of picoseconds depending on the initial rise in electron energy. As the particle temperature increase, energy exchange between the particle and its surrounding medium begins to take place through the phonon-phonon coupling, which dissipates heat across a particle-medium interface to an adjacent shell at a rate. The temperature jump at the interface of the particle and the liquid diminishes as a thermal equilibrium is achieved within ~100 ps to 1ns, depending on the liquid medium, particle size and laser pulse intensity.

Table 1. Time scale of different processes for ultrafast heating

	<100 fs	100 fs	1 ps	10 ps	100 ps	1 ns	>1 ns
Electron heating	Energy absorption by electrons						
Electron-phonon coupling		Lattice heating and increase of particle temperature					
Phonon-phonon coupling			Heat transfer from particles to its surroundings				

Simple analytical diffusive model

The characteristic time, t_0 , required for the development of a quasi-stationary temperature profile inside the particle is estimated from the formula: $t_0 \sim r_p^2 / 4\alpha_p$ where α_p is the thermal diffusivity of the solid particle. For gold nanoparticles, $\alpha_p \sim 1.2 \times 10^{-4} \text{ m}^2/\text{s}$, the characteristic time for a quasi-stationary temperature profile is $\sim 2 \text{ ps}$ for particle size of 10 nm. In many experimental cases t_0 is much smaller than the characteristic times of laser pulse duration and heating of a particle. For most of nanoparticle applications, the small size and high thermal conductivities ensures that temperature difference inside the particle is small. As a consequence, the heating of particles can be represented by one uniform particle temperature, T_p ,

$$\rho_p c_p V_p \frac{dT_p}{dt} = \frac{1}{4} I(t) K_{ab} S_p - j S_p \quad (1)$$

Where the subscript p refers to particle, t is the time, T is the temperature, ρ , c, V and S are the density, specific heat capacity, volume and surface area of the particle, I(t) is the irradiation density, K_{ab} is the absorption coefficient and j is the energy flux density removed from the particle surface that has a contribution of conduction, j_c , evaporation, j_e , and radiation, j_r .

$$j = j_c + j_e + j_r \quad (2)$$

The quasi-stationary temperature distribution around the particle in a spherical coordinate system with the origin at the particle centre under condition $t > t_T$, where $t_T \sim r_p^2 / 4\alpha_l$ is the thermal dissipation time constant, was obtained in assuming a media thermal conductivity in the form of $k = k_\infty (T/T_\infty)^a$, where a is a constant [19].

$$T(r) = T_\infty \left\{ 1 + \frac{r_p}{r} \left[\left(\frac{T_p}{T_\infty} \right)^{a+1} - 1 \right] \right\}^{\frac{1}{a+1}} \quad (3)$$

A strong temperature gradient in the surrounding media is followed from Eq. (3). The differentiation of Eq. (3) gives heat transfer across the interface and substantial heat loss from the particle into the surrounding medium can occur.

At relative low temperature, i.e. lower than the melting temperature of solid particles, the contribution of metal evaporation and radiation is small. An analytical solution can be found for equation (1) for the heating pulse, assuming a constant radiation density I and a constant thermal conductivity k_∞ for the surrounding medium [20].

$$T_p = T_\infty + \frac{IK_{ab}r_p}{4k_\infty} [1 - \exp(-Bt)] \quad (4)$$

Where r_p is the radius of the particle and $B = \frac{3k_\infty}{\rho_p c_p r_p^2}$

For the condition of $Bt_p \ll 1$, i.e. $t_p \ll t_T$, the loss of heat from the particle by heat conduction during the heating time t_p can be ignored, the expansion of the exponential function gives the maximal temperature at $t = t_p$

$$T_{\max} = T_{\infty} + \frac{3IK_{ab}t_p}{4\rho_p c_p r_p} \quad (5)$$

The cooling of the particle after the heating pulse can be written as,

$$T_p = T_{\infty} + (T_{\max} - T_{\infty}) \exp[-c(t - t_p)] \quad (6)$$

Where $c = \frac{3k_{\infty}}{\rho_p c_p r_p^2 T_{\infty}}$ and T_{\max} is the maximum temperature after the heating pulse.

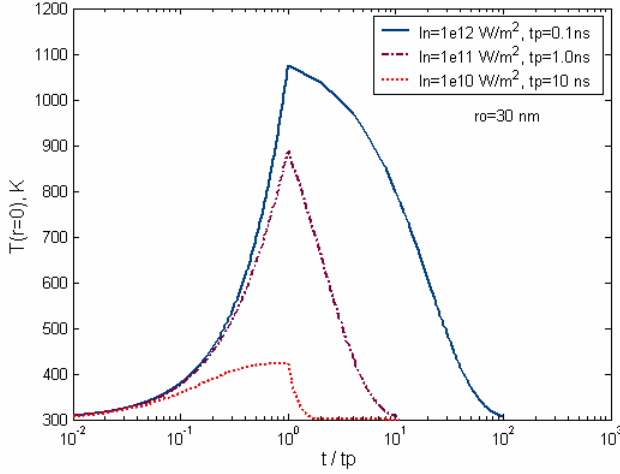


Figure 1: The effect of laser pulses on gold nanoparticle temperature surrounded by water.

Figure 1 gives an overview of gold nanoparticle temperature profile under different laser pulses, but keeping the total energy input per pulse the same. It shows clearly that the maximum temperature of particles is strongly dependent on the selection of laser parameters. The characteristic time for heat exchange between a single spherical particle and surrounding medium and the formation of quasi-stationary distribution of temperature in the medium around the particle is $t_T \sim r_p^2 / 4\alpha_l$, where α_l is the coefficient of thermal diffusivity of the medium. For gold nanoparticles of 30 nm in aqueous solution as in the simulation, the thermal relaxation time is ~ 1.3 ns. For long laser pulses, i.e pulse duration t_p exceeding the thermal relaxation time t_T , $t_p \gg t_T$, as the case shown in Figure 1, it will cause heating of both the particle and the surrounding media as heat diffuses across the particle boundary. As a consequence, the nanoparticle temperature rises rapidly at the beginning of the pulse, i.e. $t < 0.6 t_p$, but slows down significantly in the later heating period approaching asymptotically to a plateau until the completion of the laser pulse. For short laser pulse, there is practically no heat exchange between a particle and its surroundings during the pulse period. As a consequence, the laser energy is thermally confined within the particle for some period of time, causing rapid heating of the particle itself, reaching ~ 1100 K at the end of the laser pulse. For the case of $t_p \sim t_T$ as the case of $t_p = 1$ ns in Figure 2, the heating and cooling behavior is in the transition zone where the energy transfer is bounded between the regime

of thermal confinement to the regime of heat diffusion from the particle.

Discontinuous heat flow and ‘Nanobubble’

It has to be remembered that these calculations are based on pure liquid conduction with constant thermophysical properties where no phase change occurs. Nevertheless, in practical situation, the heating of a particle can be easily over the critical temperature of the surrounding liquid, which will cause strong vaporization of water near the particle surface and a vapor blanket (bubble) can be formed around the particle, termed ‘Nanobubble’ here. The generation and rapid initial expansion of these bubbles would generate a pressure wave that propagates into the tissue, which might bring a large detrimental effect to surrounding cells. The bubble dynamics such as bubble velocity and size will determine the damage range in the tissue. For nanoparticle mediated heating of cancer therapies, the formation of vapor bubble will also insulate the particle from laser radiation and surrounding liquid as soon as the bubble has been formed. The direct contact of particle with the vapor at much reduced thermal conductivity will also change significantly the heat transfer process.

The origination of vapor bubbles could be homogeneous or heterogeneous in nature. Bubble formation in liquids devoid of any impurities is termed homogeneous bubble nucleation in contrast to heterogeneous bubble nucleation which takes place. Due to the small particle sizes, it might be sufficient to consider nanoparticle suspension as homogeneous nucleation. When a liquid is heated very rapidly, a metastable state can ensue in which the liquid begins to boil at temperatures much higher than its usual equilibrium boiling point. The evaporation process can then be of an explosive nature.

Currently the detailed modelling of nanobubble is very difficult. The behaviour of the nanoparticle-vapor-water system can be described by a system of equations including heat conduction for GNPs, vapor and liquid, equation for homobaricity approximation for vapor pressure, equations for vapor pressure and mass, bubble radius, a continuity and incompressibility equations for liquid, and a bubble dynamics model with initial and boundary conditions. Different to conventional bubble phenomena, laser induced bubbles are small due to the large subcooling effect in the cell environment, i.e typically at micrometer or nanometer size, and highly transient, i.e with a life time of less than a few microseconds. It could be accompanied by strong pressure wave transportation. The systematic investigation of these phenomena is currently lacking. During the rapid expansion process of vapor bubbles, it can be assumed as inertia limited. As a very rough estimation, the Reyleigh equation will be used in the modelling of bubble dynamics, which is shown below.

$$t_b = C \sqrt{\frac{\rho(T_{\infty})}{p_s(T) - p_s(T_{\infty})}} d_b^{\max} \quad (7)$$

Where t_b is the bubble growth time, C is an empirical constant, $C=0.915$, ρ is the liquid density, $p_s(T)$ and $p_s(T_{\infty})$ are the saturation pressure of vapor at temperature T and T_{∞}

and d_b^{max} is the maximum bubble diameter and can be estimated using the energy conservation principle.

$$d_b^{max} \sim \left(\frac{6}{\pi} \frac{E}{p_\infty} \right)^{1/3} \quad (8)$$

Where E is the total energy absorbed by the particle, $E = (1 - \beta)E_{ab} = (1 - \beta)\pi r_p^2 I K_{ab} t_p$ and β is the part of energy was spent for formation of bubble and thermal energy of particle at this time instant. The bubble velocity can be estimated as

$$V_b = \left\{ \frac{2[p_s(T) - p_\infty]}{3\rho_l(T)} \right\}^{1/2} \quad (9)$$

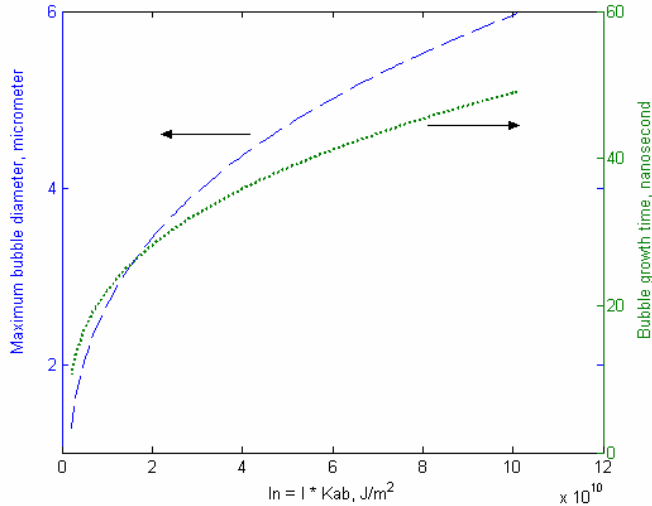


Figure 2: Estimation of bubble parameters based on Rayleigh equation ($t_p=10$ ns, $r_0=30$ nm)

Figure 2 illustrates the possible maximum bubble diameter and bubble growth time as a function of laser radiation power. In the calculation, the laser pulse length is fixed at 10 ns, which is the typical laser pulse used in conventional biomedical applications. Homogeneous nucleation temperature is generally considered to be 80% ~ 90% of the critical temperature [21], quasi-homogeneous nucleation is assumed in the calculation and the nucleation temperature is taken as 600 K when a 1-nm thick of vapor film is generated instantly around the gold nanoparticle. β is decided by calculating the energy required to bring gold nanoparticle and surrounding water of 2-nm thickness to the nucleation temperature and latent heat for bubble generation. Such a simple calculation illustrates some typical characteristic of bubbles around nanoparticles. Under such conditions, bubbles can reach their maximum diameter of a few micrometers in ~ 10 nanoseconds. Different to the pure diffusion calculation as in Figure 4, the effect of a single nanoparticle can reach a distance of a few micrometers, which is much larger than the size of particle itself and larger or comparable to typical cells. As a consequence, the generation of vapor bubbles causes a non-linear flow of heat and breaks the conventional geometry limitation of pure heat diffusion. Furthermore, the very-high bubble velocity during the bubble expansion stage, which is estimated as ~ 90 m/s for this case,

will induce a strong acoustic pressure wave considering the non-compressible nature of the surrounding liquid. These combined effects will therefore break the limitation of ‘heat localization’ and cause thermal-mechanical damage in a dimension that much large than that of a single nanopartilces. Intracellular hyperthermia therefore could achieve a similar thermal effect as that of extracellular hyperthermia.

EXAMPLE EXPERIMENTAL STUDY

Controlled synthesis of nanomaterials

Due to the excellent thermal-physical properties, low cytotoxicity and good biocompatibility, as well as prior clinical experience of gold-based pharmaceuticals (FDA approved), gold nanoparticles (GNP) could become an excellent potential candidate for NPUT, and will be the focus of this study. Not only suitable for medical purposes, ultrasound has been shown to have unique capability in fabricating nanoparticles and nanostructured materials, associated with the cavitation effect. Controlled colloidal nanoparticles, including Au, Ti, Pt, Pd, Fe, MnO_2 , and CdS, have been produced ultrasonically through the reduction of metal salts or metal complexes. In this study, different sized spherical-shaped gold nanoparticles will be fabricated by the citrate reduction method, with the aid of an ultrasonic device. The detailed study has been recently reported in [22], where gold nanoparticles with different size and shapes have been successfully synthesized through the aid of ultrasound irradiation.

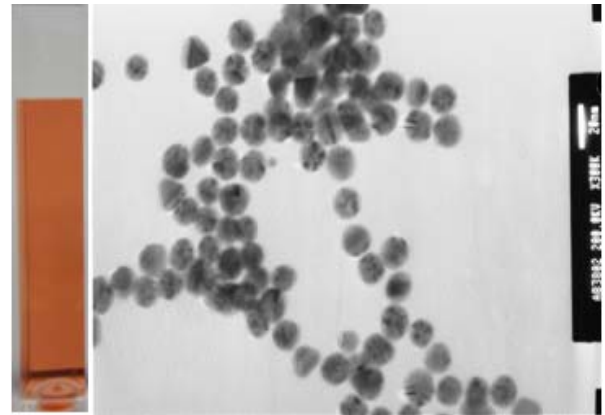


Figure 3: TEM image of spherical-shaped gold nanoparticles and resultant dispersion color (left)

The primary size and shape of nanomaterials are identified by a transmission electron microscopy (TEM) and a scanning electron microscope (SEM) equipped with an Energy Dispersive X-ray spectroscope (EDX). The particle size distribution in liquid was identified by a dynamic light scattering device (Malvern nanosizer). The crystal structure and elemental information was provided by x-Ray Diffraction Spectroscopy. Ultra-violet (UV) spectroscopy is used to measure the light absorption rate. Examples of synthesized particles and their size distribution in shown in Figure 3. The average size of the gold nanoparticles observed is approximately 15nm to 20nm in diameters and the shape of

gold nanoparticles is spherical. The particle size distribution in the liquid phase is measured by the dynamic light scattering (DLS) method. A narrow size-distribution is found, typically in the range of 10~30 nm. With the application of ultrasonication during the synthesis, the particle size becomes smaller, reducing from ~ 20nm to 16nm measured by Zetasizer based on the DLS method.

Effective thermophysical properties of nanoparticle suspensions

Proper understanding of the properties of nanoparticle suspensions is fundamental for the heating effect. For a simple estimation, the homogeneous approach can be applied that only consider the effective properties of nanoparticle suspensions, while neglecting detailed interaction among nanoparticle, and between nanoparticle and surrounding liquid. For heating under EM field, the specific absorption rate (SAR) of a nanoparticle suspension is then related to the electric conductivity and permittivity through:

$$SAR = \frac{\sigma(\omega) \langle P \rangle |E|^2}{2P_{\max} \rho} \sim \varepsilon'' \varepsilon_0 \omega^3 B_1^2, \text{ where } P \text{ is the RF power,}$$

ρ is the tissue density, E is the electric field strength, B_1 is the EM amplitude, ω is the EM frequency, ε'' and ε_0 are the imaginary permittivity and free space permittivity respectively. Consequently for EM-nanoparticle heating applications, the main properties of interests are thermal conductivity, electrical conductivity, specific heat and permittivity, as well as the interfacial properties such as surface tension and wettability at higher heating power where bubbles are likely formed. For non-EM application such as ultrasound heating, the major influential parameters are similar but excluding the electrical conductivity and permittivity.

The effective thermal conductivity of produced nanoparticle suspension is measured by a transient hot-wire method, and shown in Figure 4. With the increase of particle concentrations, the effective thermal conductivities of gold nanofluids increase, exhibiting a non-linear trend, i.e., the increase is small at low concentrations but becomes significantly at over 33.31 $\mu\text{M/l}$. It also shows that the effective thermal conductivity, k_{eff} , is significantly affected by particle size. As the specific surface area increases with the decrease of particle size, it is expected that k_{eff} would be higher at low particle dimensions. This is true when we compare the gold nanofluids containing 10-nm spherical nanoparticles with that of 60-nm gold nanoplates. However when we compare the results of the 250-nm gold plates with that of spherical particle nanofluids, a reverse trend is obtained. The thermal conductivities of nanofluids containing 250-nm gold nanoplate is always higher than that of 15-nm spherical particles. The particle at the concentration of 764 $\mu\text{M/L}$ reaches approximately 1.0 and 0.8 W/mK, respectively, for 250-nm gold plates and 15-nm spherical particles. Such a result shows that apart from the particle size, particle shape also plays a significant role in determining the effective thermal conductivity. While the effect of shape is small at low particle concentrations, it signifies its influences as the concentration increases. Qualitatively, such a

result is consistent with a few other studies. Recently, the International Nanofluid Properties Benchmark Exercise (INPBE) showed that the effective thermal conductivities of alumina nanorod nanofluids (80 nm in length and 10 nm in diameter) were 45% and 30% higher than that of 10-nm spherical alumina nanofluids at concentrations of 3% and 1% volume fraction of nanomaterials, respectively [23]. A few other studies have also reached similar results [24].

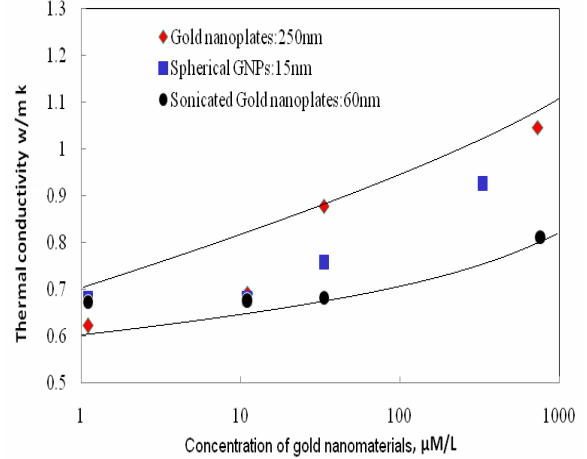


Figure 4: Effective thermal conductivity of GNP dispersions [22]

Using a variable frequency probe, our initial measurement on the electrical conductivity of gold nanosuspensions shows that the electrical conductivity is strongly dependent on the frequency within the experimental range, 100 MHz ~ 10 GHz.

Bulk heating effect of GNP dispersions

Both EM heating and ultrasonic heating of GNP samples were conducted in the experiment. Spherical shaped gold nanoparticles in the size range of 10 ~ 300 nm were diluted to four concentrations (11.1 $\mu\text{M/L}$, 33.3 $\mu\text{M/L}$, 75 $\mu\text{M/L}$, 150 $\mu\text{M/L}$). For ultrasonic heating, the samples were held in transparent cuvettes, controlled at 50ml each, and were fixed inside a water bath. The heating was introduced by an ultrasonic device having a frequency of 60kHz, positioned at the bottom of the liquid bath. Each experiment was conducted for 5mins, where the transient temperature increase of the nanoparticle dispersion was measured by one thermocouple immersed inside the dispersion, and logged into a PC through a Data Acquisition System (DAQ). Each sample was repeated at least 3 times.

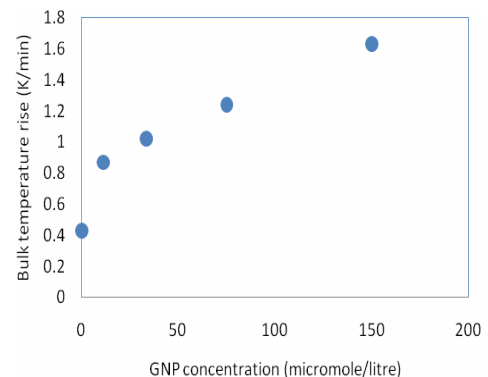


Figure 5: Average bulk heating rate under an ultrasonic irradiation field

Figure 5 shows the temperature increase of the bulk liquid in four different gold nanoparticle concentrations, which are 11.1 μ M/L, 33.3 μ M/L, 75.0 μ M/L and 150 μ M/L. It clearly shows that small concentrations of gold nanoparticles can increase significantly the heating rate of the base fluid. The bulk fluids temperature increases nearly linearly with the ultrasonic irradiation time. The temperature rise rate increases with the increase of GNP concentrations. Nearly four times increase in the heating rate is achieved at a GNP concentration of 150 μ M/L.

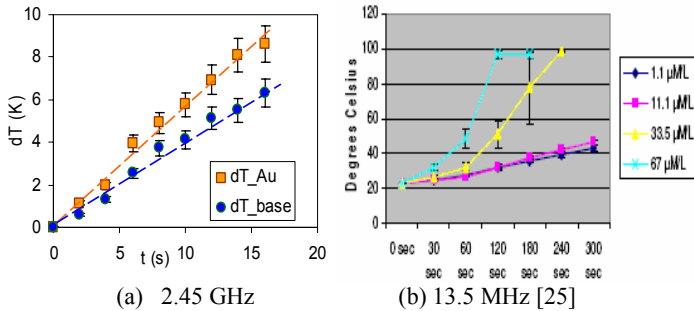


Figure 6: Bulk heating of GNP under different frequencies of electromagnetic field

Some preliminary heating result under different frequencies of EM spectrum has been conducted, as one example is shown in Figure 6. Due to the different frequency used, the heating result is different to some previous reported results [25], which reveal a frequency-dependent heating behaviour of gold nanosuspensions. Non-uniform energy distribution is also revealed through a numerical simulation. The particle size effect is unclear at moment. Only two reports can be found in open literature on the effect of particle size, both using GNPs and heated under an EM frequency of 13.56 MHz, but totally different results were reported. For instance, the absorption rate of GNPs is found to increase with the particle size, i.e., compared with 2 nm GNPs, the absorption efficiency increased by ~ 50 times, ~ 1800 times and ~ 5600 times for GNPs with particle size of 5 nm, 10 nm and 20 nm respectively [26]. Bulk-solution heating rates were found to be in the range of 4.5 to 7.6 $^{\circ}$ C per minute by using 200 W of EM input power. It was suggested that an optimum in absorption efficiency occurred near 10 nm size. Such a result contrasted significantly to that of Moran et al. [7] even under the same heating frequency, where it reported that the specific absorption rate increased with the decrease of nanoparticle size, which is due to a pure Joule-heating effect associated with the increased electrical resistance at low particle dimensions. It appears that more fundamental studies are urgently needed. However these limited studies did show that the heating rate is dependent on the EM frequency, particle materials and particle size, as well as a non-linear increase in temperature with the increase in concentration [25], i.e. a significant temperature rise is only achieved above a critical particle concentration, whereas the heating effect is small for lower particle concentrations, which provides an

opportunity to minimize the heating due to off-targeted nanoparticles.

DISCUSSION

It should be noted that the only difference between the base DI water and different nanoparticle dispersions is the existence of nanoparticles, which illustrates that the different heating effect shown in section 3.2 could only be caused by nanoparticles. These experiments clearly reveal that the introduction of nanoparticles could focus ultrasonic irradiation and EM energy much more rapidly than that of pure water. Different nanomaterials have different effects whereas gold nanoparticles possess greater capability than other materials tested.

It is still unclear on the reasons of increased heating rate. For instance if considered only by conduction, i.e.,

$$\frac{\partial T}{\partial t} = \frac{k \partial^2 T}{\rho c \partial x^2}$$

, the transient temperature increase rate should be proportional to the effective thermal conductivity. To achieve the a 4-times increase in the heating rate as shown by 150 μ M/L gold dispersion, a four-fold increase in thermal conductivity is required if all the heating effect comes from thermal conduction. The result shown in Figure 4 clearly shows that the maximum thermal conductivity increase was found to be $\sim 60\%$, occurred at the highest concentration, 760 μ M/L. It is apparent that the increase in thermal conductivity should not be fully responsible for the rapid temperature increase. An increased cavitation effect due to the presence of nanoparticles should be responsible for enhanced ultrasound absorption. For EM absorption enhancement by GNP, much debate has been ongoing. Detailed examinations of the effect of different materials and the reasons on the rapid temperature increase are currently still ongoing.

Section 4 and 5 clearly shows the potential large difference between local temperature around heated nanoparticles and the average bulk temperature. Compared with potential rapid heating of individual nanoparticles, the average bulk temperature rise is much slower. Experimentally temperature at nanoscale can be obtained by either by laser approach (i.e. in a pump-probe configuration) or AFM-based method (i.e. Scanning Thermal Microscope). However the detailed local temperature in a liquid carrier is difficult to measure due to the size of particles involved. A recently study reveals experimentally that the heating of nanoparticles can be used effectively controlling ion channels and neurons [27]. The local temperature information was obtained by bonding temperature-dependent fluorescence particles onto the nanoparticle surface, where a colour change was recorded to give a collective temperature effect of many nanoparticles. Though not at individual nanoparticle level, the study did reveal big temperature difference between the liquid phase and an averaged nanoparticle temperature. A further understanding of the heating of nanoparticles in-situ and thermal response at nanoscale, which is essential for successful medical applications, call for a cross-disciplinary collaboration among engineers, scientists and clinicians.

SUMMARY

This work reviews some nanoparticle-associated thermal therapies and proposes a systematic study of remote-controlled nanoparticle heating for medical applications. Preliminary theoretical and experimental studies are conducted to reveal the potentials of this exciting field. In view of the scope of the study, a few general comments can be made,

- Nanoparticle associated thermal phenomena is fundamental to a number of biomedical applications
- Both theoretical and experimental studies have shown that significant localized temperature rise can be achieved.
- Two type of nanoparticle heating is identified, i.e. continuous and non-discontinuous heating models depending on the intensity of external heating source.
- Analytical study shows that formation of nanobubbles has an explosive nature. The rapid formation and contraction of bubbles around heated nanoparticles, associated with the propagation of pressure waves, could bring thermal-mechanical damage to surrounding cells at a dimension much larger than that of a nanoparticle
- Bulk heating experiments show that that GNP is an excellent agent to focus ultrasound irradiation and EM energy, which could be an ideal candidate for medical applications.

Further understanding of the heating of nanoparticles in-situ and thermal response at nanoscale, which is essential for successful medical applications, call for a cross-disciplinary collaboration among engineers, scientists and clinicians.

ACKNOWLEDGEMENT

The authors would like to extend his thanks to EPSRC for their financial support under Grant No: EP/E065449/1, and Ms Hui-Juan Chen of Queen Mary University of London for nanoparticle synthesis.

REFERENCES

- [1] Malam Y, Loizidou M, Seifalian AM. Liposomes and nanoparticles: nanosized vehicles for drug delivery in cancer. *Trends in Pharmacological Sciences* 30 (11), 592-599, 2009
- [2] Will O, Purkayastha S, Chan C, et al. Diagnostic precision of nanoparticle-enhanced MRI for lymph-node metastases: a meta-analysis *Lancet Oncology* 7(1), 52-60, 2006
- [3] Hergt R, Dutz S et al., Magnetic particle hyperthermia: nanoparticle magnetism and materials development for cancer therapy. *J. Phys.: Condens. Matter* 18 S2919, 2006
- [4] Huang X, Jain P K, El-Sayed M. Plasmonic photothermal therapy (PPTT) using gold nanoparticles *Lasers in Medical Science* 23, 217-228, 2008
- [5] Hilger I et al. Electromagnetic heating of breast tumors in interventional radiology: in-vitro and in-vivo studies in human cadavers and mice. *Radiology*, 218: 570-5, 2001
- [6] Hergt R., Hiergeist R et al. *J. Magn. Magn. Mater.* 270, 345. 2004
- [7] Moran C, Wainerdi S et al.. Size-dependent joule heating of gold nanoparticles using capacitively coupled radiofrequency fields. *Nano Research*, 2 (5): 400-405 2009
- [8] Skirtach A et al. Nanorods as wavelength selective absorption centers in the visible and Near infrared regions of the electromagnetic spectrum. *Adv. Materials*, 20: 506-10, 2008
- [9] Cobley C, Au L, Chen J et al. Targeting gold nanocages to cancer cells for photothermal destruction and drug delivery *Expert Opinion on Drug Delivery* 7, 577-587, 2010
- [10] Zquez E and Prato M Carbon Nanotubes and Microwaves: Interactions, Responses, and Applications *ACS Nano*, 3 (12), 3819-3824, 2009
- [11] O'Neill BE, Vo H et al. Pulsed high intensity focused ultrasound mediated nanoparticle delivery: mechanisms and efficacy in murine muscle. *Ultrasound Med Biol.* 35(3):416-24. 2009
- [12] Zeisberger M., Dutz S. et al., *J. Magn. Magn. Mater.* 311, 224, 2005
- [13] Kalambur V, Longmire E, Bischof J Cellular level loading and heating of superparamagnetic iron oxide nanoparticles. *Langmuir* 23, 12329-12336. 2005
- [14] Smith M. J., Ho V. H. B., Darton N. J., Slater K. H., Effect of magnetite nanoparticle agglomerates on ultrasound induced inertial cavitation, *Ultrasound in Medicine & Biology*, 35 (6):1010-1014, 2008
- [15] Ho V. H. B., Smith M. J., Slater K. H., Effect of magnetite nanoparticle agglomerates on the destruction of spheroids using high intensity focused ultrasound, *Ultrasound in Medicine & Biology*, 37(1):169-175, 2010
- [16] Lin C. Y., Huang Y. L., Li j. R., Chang F. h., Lin W. L., Effects of focused ultrasound and microbubbles on the vascular permeability of nanoparticles delivered into mouse tumors, *Ultrasound in Medicine & Biology*, 36(9):1460-1469, 2010
- [17] Chen H J and Wen D S. Nanoparticle-mediated ultrasonic heating for biomedical applications. *Thermal and Materials Nanoscience and Nanotechnology* Turkey, 2011
- [18] Wen D S Intracellular hyperthermia: nanobubbles and their biomedical application. *Int J Hyperth*, 25(7):533-541, 2009
- [19] Pustovalov VK, Bobuchenko DS. Heating, evaporation and combustion of a solid aerosol particle in a gas exposed to optical radiation. *Int J Heat Mass Trans;*32:3-17. 1989
- [20] Pustovalov V. Theoretical study of heating of spherical nanoparticle in media by short laser pulses. *Chem Phys*, 308:103-108. 2005
- [21] Kotaidis V, Dahmen C, Plessen G, Springer F, Plech A. Excitation of nanoscale vapor bubbles at the surface of gold nanoparticles in water. *J Chem Phys* 2006;124:184702.
- [22] Chen H J and Wen D S Ultrasound-aided fabrication of gold nanofluids, *Nanoscale Research Letters*, 6:198, 2011
- [23] Buongiorno J, Venerus D, et al.: A benchmark study on the thermal conductivity of nanofluids. *J Appl Phys*, 106:0943122009
- [24] Timofeeva EV, Routbort JL, Singh D: Particle shape effects on thermophysical properties of alumina nanofluids. *J Appl Phys* 2009, 106(014304):1-10.
- [25] Gannon C, Patra C R, Bhattacharya R, Mukherjee P and Curley S. Intracellular gold nanoparticles enhance non-invasive radiofrequency thermal destruction of human gastrointestinal cancer cells. *Journal of Nanobiotechnology*, 6: 2008
- [26] Kruse D, Stephens D et al. (2009). Absorption of radiofrequency electromagnetic energy by gold nanoparticles for thermally-activated local drug delivery. *2009 World molecular imaging congress*, US
- [27] Huang, H, Delikanli S, Zeng H, Ferkey D and Pralle A. Remote control of ion channels and neurons through magnetic-field heating of nanoparticles. *Nature Nanotechnology*, 5, 602-606, 2010